Journal of Global Positioning Systems (*2022*)

Vol. 18, No. 1: 28-40

DOI: 10.5081/jgps.18.1.28

Journal of Global Positioning Systems

2022

A Geometry-based Ambiguity Validation (GBAV) Method for GNSS carrier phase observation

Wu Chen[1), 4)], Ying Xu[2)], Duojie Weng[1),4)], Shengyue Ji[3)]

[1)] Department of Land Surveying and Geo-informatics, Hong Kong Polytechnic University

[2)] College of Geomatics, Shandong University of Science and Technology, Qingdao, China

[3)] School of Geosciences, China University of Petroleum, Qingdao, China

[4)] Research Institute for Artificial Intelligence of Things, Hong Kong Polytechnic University

✉ **Corresponding author**: Wu Chen, lswuchen@polyu.edu.hk

Abstract: Integer ambiguity validation is an indispensable and critical step in GNSS carrier phase positioning for precise and reliable positioning applications. The crucial problems associated with any ambiguity validation methods are as follows. 1) The fixed ambiguity vector can be separated from all other ambiguity candidates under certain tests (separability). 2) The probability of fixing to wrong ambiguity combinations (mis-fixing) can be controlled to an acceptable level based on different application requirements. Traditional ambiguity validation methods, such as the *R*-ratio and the difference tests which use one statistical test to control both separability and mis-fixing rate, are widely used due to easier computation. The performances of these methods are generally acceptable. However, experiments show that these tests with a fixed threshold can cause either a small percentage of mis-fixing or overly conservative with long observation time. In this paper, we propose a new Geometry Based Ambiguity Validation (GBAV) method which uses two statistical tests to control geometry separability and mis-fixing probability separately. The thresholds for both tests can be strictly determined based on user requirements to control the quality of ambiguity resolution. Three 24-hour GNSS (GPS, BDS) datasets (two short baselines and one middle-range baseline) are processed using the proposed GBAV method, and compared with the popular *R*-ratio method. The results show that by giving proper control on the mis-fixing probability (<0.01%), there is no mis-fixing case in all three datasets.

Keywords: GNSS, Ambiguity, Carrier Phase

1. Introduction

The Global Navigation Satellite Systems (GNSS) are satellite navigation systems which provide space-based positioning, navigation and timing (PNT) services in all weather conditions, anywhere on or near the Earth (Leick 2004). GNSS provides two common types of measurements for positioning, namely pseudo-range and carrier phase. These measurements enable the determination of the ranges between the receiver antenna and the satellites. The carrier phase based positioning results in more precise range than those from pseudo-range, if the carrier phase ambiguity can be reliably resolved (Han and Rizos 1999). However, an incorrect integer ambiguity solution may cause severe biases in the position solution and in any other of the real-valued parameters and it is important to assess the probability of correct ambiguity estimation (Verhagen and Teunissen 2013). Thus, integer ambiguity validation is an indispensable and critical step in GNSS ambiguity resolution process. Over the past years, various ambiguity validation methods have been proposed, such as *F*-ratio test (Frei and Beutler 1990; Euler and Landau 1992), *R*-ratio test (Euler and Schaffrin 1991; Leick 2004; Teunissen and Verhagen 2009), difference test (Tiberius and De Jonge 1995), projector test (Wang et al. 1998; Han 1997). These methods are easy to compute and the performances are generally acceptable, if correct critical values are selected. However, there are some disadvantages for this type of ambiguity validation methods. Taking the most popular ratio test as an example, the critical values are normally selected empirically, as the statistic distributions for the tests are difficult to be established.

Editor in charge: Dr. Dongsheng Zhao

Therefore it is difficult to evaluate or to compare the performances of these empirical tests (Li and Wang 2012). In addition, the experiments results from (Teunissen and Verhagen 2009; Teunissen and Verhagen 2004; Teunissen 2013;Verhagen and Teunissen 2013) indicated that the traditional use of the ratio test with a fixed threshold often results in either unacceptably high failure rates or overly conservative. For the strong models, the fixed value ratio tests are often too conservative, so that the false alarm rates are unnecessarily high, while the failure rates are very close to zero. For weak models, on the other hand, the currently used fixed values are often too low, so that the fixed solution is often wrongly accepted, resulting in high failure rates. To overcome these problems, Verhagen and Teunissen (2006) proposed a model-driven ratio test with a fixed failure rate. Simulation results have shown that it is possible to describe the threshold values based only on the number of ambiguities and the failure rate. Besides the ambiguity validation test mentioned above, Ellipsoidal Integer Aperture (EIA) (Teunissen 2003), and Penalized Integer Aperture (PIA) (Teunissen 2004) based validation methods are dependent on lower bound (Teunissen 1998a) or upper bound (Teunissen 2000) of ambiguity resolution success rates. The advantage of these approaches is that critical values of the statistical tests are linked with user controlled fail rates. However, the critical values rely on satellite geometry and it is difficult to describe them mathematically, particularly for multiple epoch observations. Also, the sample size is important for these approaches, resulting that longer observation time is preferred for reliable solution (Li and Wang 2012). To reduce the time required for observation and to improve the reliability, Ji et al. (2010) proposed to combine *R*-ratio and EIA tests together for ambiguity validation. Through allowing slight overlap of pull-in region, the observation time for EIA could be significantly reduced. The *R*-ratio test was applied at the same time to discriminate the cases in the overlapping regions. Test results showed the combined validation method improved the ambiguity resolution reliability, and had similar efficiency to the *R*-ratio at the same time. A comprehensive review and evaluation of these tests can be found in Verhagen (2004; 2005), Verhagen and Teunissen (2006), and Li and Wang (2012).

Geometrically, ambiguity resolution tries to find an intersection point of all ambiguities with minimum residuals, compared with all the other ambiguity combinations in ambiguity space. If there are no errors in GNSS measurements, the ambiguities can be fixed to integers when there is only one intersection point. For a given GNSS datasets, if there were two intersection points, no validation method can distinguish them. On the other hand, the measurement errors may shift the correct intersection point significantly. It will cause the ambiguity resolution algorithms fixing to wrong ambiguity. As mentioned above, ratio tests were applied popularly and empirically. They use one statistical test to control both problems. As a result, these tests with a fixed threshold may cause some ambiguity mis-fixing casesor overly conservative with long observation time. In this paper, we proposed a new Geometry Based Ambiguity Validation (GBAV) method to separate the validation test into statistical tests, including the spatial separability and mis-fixing rate. Based on the statistical distributions of the two tests, we are able to determine the thresholds based on user requirements to control the spatial separability and mis-fixing rate separately. With this new method, we can efficiently control the mis-fixing probability to ensure the quality of ambiguity resolution.

In section 2, the concept spatial separability and mis-fixing condition are introduced and their associated probabilities are given. The proposed Geometry Based Ambiguity Validation (GBAV) method is summarized in section 3. Numerical tests and results with three GNSS 24-hour datasets are given in section 4. The discussions and conclusions are given in section 5.

2. Spatial Separability and Mis-fixing Condition for Ambiguity Validation

The general form of linear observation equation on GNSS carrier phase observation can be expressed as (Parkinson et al. 1996; Leick 2004; Hofmann-Wellenhof et al. 1993):

$$AX + BN + \varepsilon = L \tag{1}$$

where L denotes the double difference observation vector, N is double difference carrier phase integer ambiguity vector ($N \in Z^n$), X is the vector of the other unknown parameters (including position coordinates), ε is the random errors, and the matrices A and B are the corresponding design matrices.

The solution of Eq. (1) can be obtained by minimizing Eq. (2) (Verhagen 2004):

$$\min ||L - BN - AX||^2_{Q_L}, \quad N \in Z^n, X \in R^n \tag{2}$$

where $||*||^2_{Q_L} = (*)^T {Q_L}^{-1}(*)$, and Q_L is the variance-covariance matrix of observation vector L.

In general, the ambiguity fix solution can be divided into three steps (Teunissen 1995). In the first step, the integer constraints on the ambiguities are simply ignored. The unconstrained least-squares solution is referred to as the float solution of $\hat{N}$, $\hat{X}$. The corresponding variance-covariance (VC) matrix is as following,

$$\begin{bmatrix} \hat{N} \\ \hat{X} \end{bmatrix}, \begin{bmatrix} Q_{\hat{N}} & Q_{\hat{N}\hat{X}} \\ Q_{\hat{X}\hat{N}} & Q_{\hat{X}} \end{bmatrix} \quad (3)$$

In the second step, the integer ambiguity estimation $\breve{N}$ is computed from the 'float' ambiguity, subject to $\min ||\hat{N} - \breve{N}||^2_{Q_{\hat{N}}}$. Integer rounding, integer bootstrapping and integer least-squares are different methods for obtaining the integer solution. Integer least-square (ILS) is optimal, as it maximizes the probability of correct integer estimation (Teunissen 1999). In contrast to rounding and bootstrapping, an integer search is needed to compute the ILS solution. This can be efficiently done with the LAMBDA method (Teunissen 1995b). Finally, fixed solution is obtained by:

$$\breve{X} = \hat{X} - Q_{\hat{X}\hat{N}} Q_{\hat{N}}^{-1} (\hat{N} - \breve{N}) \quad (4)$$

For relative positioning, if the double difference ambiguity vector is truly known as N_0, the double difference carrier phase observation equation can be written as,

$$AX_0 = L_0 + \lambda N_0 + e \text{ with a weight matrix } P \quad (5)$$

where A is the design matrix, X_0 is the receiver position vector, L_0 is the double difference carrier phase measurement vector without noise, λ is the wavelength of carrier phase, and e is the true error vector of carrier phase measurement. The other errors, such as tropospheric delay and ionospheric delay are not considered here as the double difference process significantly reduces their effects on short baselines. For Long baselines, we can use GNSS measurements to estimate tropospheric and ionospheric delays, together with receiver position and clock error parameters.

Assuming N_0 is known, the residual vector V_0 and the weighted sum of squared residuals Z_0 of Eq. (5) can be expressed as Eqs. (6) and (7), when the least squares estimation method is used to estimate position vector X_0.

$$V_0 = (I - H)e \quad (6)$$

$$Z_0 = V_0^T P V_0 = e^T (I - H) P (I - H) e \quad (7)$$

where

$$H = A(A^T P A)^{-1} A^T P \quad (8)$$

The ambiguity validation problem can be generally described as follows.

Give a group of ambiguity candidates $(N_1, N_2, N_3, \dots \dots . N_m)$, and $N_0 \epsilon (N_1, N_2, N_3, \dots \dots . N_m)$, $\forall N_i \epsilon (N_1, N_2, N_3, \dots \dots . N_m)$, check if $N_0 = N_i$ for all $i = 1, \dots \dots, m$.

If N_i is a selected candidate,

$$AX_i = L_0 + \lambda N_i + e = L_0 + \lambda N_0 + \lambda \Delta N_i + e \quad (9)$$

where

$$\Delta N_i = N_i - N_0 \quad (10)$$

The total error in Eq. (9) is

$$\Delta = \lambda \Delta N_i + e \quad (11)$$

The residual vector of Eq. (9) is

$$V_i = (I - H)\Delta = \lambda (I - H) \Delta N_i + (I - H) e \quad (12)$$

The weighted sum of squared residuals Z_i is

$$Z_i = V_i^T P V_i = \lambda^2 \Delta N_i^T (I - H) P (I - H) \Delta N_i + e^T (I - H) P (I - H) e + 2\lambda \Delta N_i^T (I - H) P (I - H) \mathrm{e} \quad (13)$$

On the other hand, differencing Eq. (5) and Eq. (9), we can have:

$$A \Delta X_i = \lambda \Delta N_i \quad (14)$$

where $\Delta X_i = X_i - X_0$ is the position shift due to the wrong ambiguity.

There is no measurement error in Eq. (14), its residual only reflects the coordinate difference caused by the ΔN_i. The residual and the weighted sum of squared residuals of Eq. (14) are,

$$V_{\Delta Ni} = \lambda (I - H) \Delta N_i \quad (15)$$

and

$$V_{\Delta Ni}^T P V_{\Delta Ni} = \lambda^2 \Delta N_i^T (I - H) P (I - H) \Delta N_i \quad (16)$$

In another word, the residuals of Eq. (14) only reflect whether N_0 and N_i can be separated geometrically or not. For instance, N_0 and N_i cannot be separable if $V_{\Delta Ni} = 0$. Furthermore, the weighted sum of squared residuals (Eq. 16) can also be used to describe the degree whether N_0 and N_i can be separated. When $V_{\Delta Ni}^T P V_{\Delta Ni}$ is too small compared to $V_0^T P V_0$; N_0 and N_i cannot be separated geometrically. Conversely, it is possible to separate N_0 from N_i while $V_{\Delta Ni}^T P \mathrm{V}_{\Delta Ni}$ is relatively larger than the sum of the squares of noise $V_0^T P V_0$.

Inserting Eqs. (6), (7), (15) and (16) into (13),

$$Z_i = V_i^T P V_i = V_{\Delta Ni}^T P V_{\Delta Ni} + V_0^T P V_0 + 2 V_{\Delta Ni}^T P V_0 \quad (17)$$

The weighted sum of squared residuals for Eq. (9) consists of three terms. The first term is only determined by the difference of selected ambiguity vector and the true ambiguity vector. The second term is only related to the true error e, and the third term is affected by the projection of the true error to the direction of residual vector $V_{\Delta Ni}$.

If the ambiguity candidates $(N_1, N_2, N_3, \dots \dots . N_m)$ of Eq. (9) is arranged based on the size of weighted sum of squared residuals (Eq. (13)), from smallest to the largest, the ambiguity N_1 is an optimal solution of Eq. (9). Thus the ambiguity validation problem can be described as whether N_1 is the true ambiguity vector N_0 or not, which can be divided into two cases: 1) N_0=N_1, and 2) N_0=N_i ($i \neq 1$).

Case 1: N_0=N_1,

Let us consider case 1 first, when N_1 is the true ambiguity vector, or,

$$N_0 = N_1 \tag{18}$$

and thus,

$$V_1 = (I - H)e \tag{19}$$

Select N_i as a possible candidate ($i \neq 1$), the difference of the sums of residuals between N_1 and N_i should be,

$$\Delta Z_{1i} = Z_i - Z_1 = V_{\Delta N1i}^T P V_{\Delta N1i} + 2V_{\Delta N1i}^T P (I - H)e = V_{\Delta N1i}^T P V_{\Delta N1i} + 2V_{\Delta N1i}^T P V_1 > 0 \tag{20}$$

where $\Delta N_{1i} = N_i - N_1$

In Eq. (20), the first term is determined only by the geometry of satellites and ambiguity difference ΔN_{1i}. As mentioned above, it can be used to describe whether N_0 (N_1 in this case) and N_i can be separated compared to $V_0^T P V_0$ ($V_1^T P V_1$in this case). Now we can define the separability index of N_i and N_1 as:

$$S_{1i} = \frac{V_{\Delta N1i}^T P V_{\Delta N1i}}{V_1^T P V_1} \tag{21}$$

When S_{1i} is relatively large, N_1 and N_i are geometrically separable compared with a given noise level $V_1^T P V_1$. Thus, the geometrical separability condition of ambiguity resolution is:

$$S_{1i} = \frac{V_{\Delta N1i}^T P V_{\Delta N1i}}{V_1^T P V_1} > k1 \tag{22}$$

The next question is how to determine k1. Since the distribution of the GNSS satellites can be considered as random, $V_{\Delta N1i}$ should obey the normal distribution just like the V_1 (Teunissen 1998b). Although we are not able to prove this hypothesis at moment, simulation tests are carried out to test if the distribution of $V_{\Delta N1i}$ is Gaussian. In the simulation, we firstly calculate three data sets of $V_{\Delta N1i}$ and consider them as the samples using the observation collected for the experiments (see section 4) in this study. The numbers of the samples are 34648. The probability density of one set of $V_{\Delta N1i}$ is shown in Fig 1 (the blue line). The mathematical expectation (μ) and standard deviation (σ) of $V_{\Delta N1i}$ is 0.000 and 0.025 respectively. The black line shows the normal probability density function with the same μ and σ. As shown in Fig 1, these two lines are very closer to each other. Furthermore, we apply the Jarque-Bera test in Matlab, h = jbtest(x), which returns a test decision for the null hypothesis that the data in vector x comes from a normal distribution. The alternative hypothesis is that it does not come from such a distribution. The result h is 1 if the test rejects the null hypothesis at the 5% significance level, and 0 otherwise. Test shows that all the three samples come from a normal distribution. As the molecular and denominator of Eqs. (21) is independent, S_{1i} obeys F-distribution, $S_{1i} \sim F(d, d)$, d is the degree of freedom. Thus, by giving a significant level, $k1$ is uniquely determined by the distribution of $S_{1i} \sim F(d, d)$.

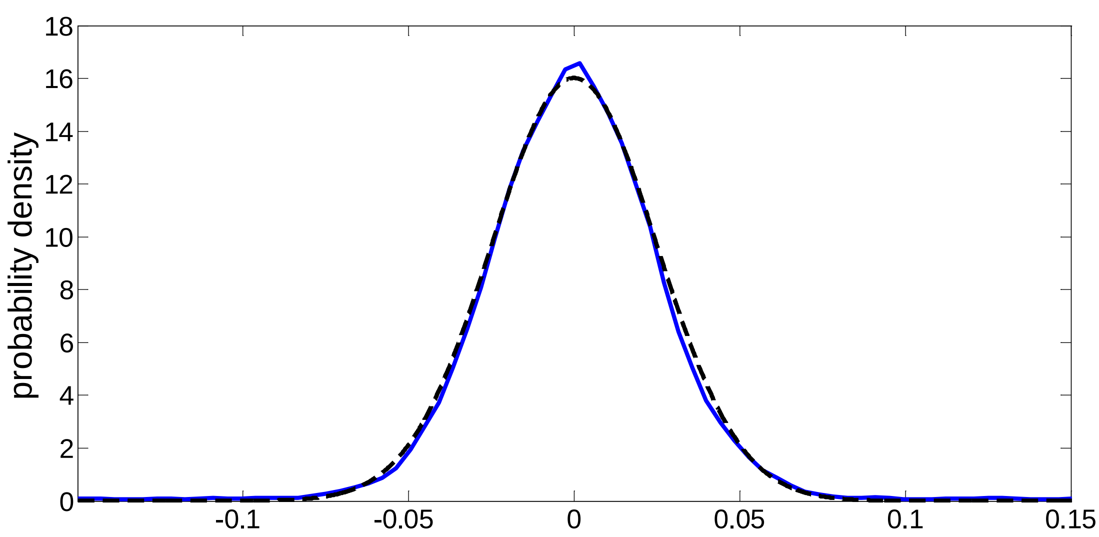

Fig 1 The distribution of $V_{\Delta N1i}$ (sample one, blue line), The Normal Distribution (black line)

The second term in Eq. (20) is determined by the size of residual of the true error e. From Eq. (20), we can get

$$\frac{2V_{\Delta N1i}^T P(I-H)e}{V_{\Delta N1i}^T PV_{\Delta N1i}} = \frac{2V_{\Delta N1i}^T PV_0}{V_{\Delta N1i}^T PV_{\Delta N1i}} > -1 \quad (23)$$

We define $M_i = m \cdot V_i, m = \frac{2V_{\Delta N1i}^T P}{V_{\Delta N1i}^T PV_{\Delta N1i}}$, and $M_0 = \frac{2V_{\Delta N1i}^T PV_0}{V_{\Delta N1i}^T PV_{\Delta N1i}} = \frac{2V_{\Delta N1i}^T P(I-H)e}{V_{\Delta N1i}^T PV_{\Delta N1i}}$.

In case 1, $V_1 = (I-H)e$, so

$$M_1 = M_0 = \frac{2V_{\Delta N1i}^T PV_1}{V_{\Delta N1i}^T PV_{\Delta N1i}} = \frac{2V_{\Delta N1i}^T PV_0}{V_{\Delta N1i}^T PV_{\Delta N1i}} > -1 \quad (24)$$

If the measurement error vector e obeys a zero mean normal distribution, M_0 also obeys normal distribution, as it is a linear combination of error vector e.

Case 2: N_0=N_i ($i \neq 1$).

Let us consider the second case now, when N_i ($i \neq 1$) is the true ambiguity vector ($N_0 = N_i$). If N_1 is selected as an ambiguity solution in this case (with the smallest sum of residuals), an ambiguity mis-fixing happens.

In this case,

$$V_i = (I-H)e \quad (25)$$

$$V_1 = \lambda(I-H)\Delta N_{i1} + V_i = -V_{\Delta N1i} + V_i \quad (26)$$

$$\Delta Z_{1i} = Z_i - Z_1 = -V_{\Delta Ni1}^T PV_{\Delta Ni1} - 2V_{\Delta Ni1}^T P(I-H)e = -V_{\Delta N1i}^T PV_{\Delta N1i} + 2V_{\Delta N1i}^T P(I-H)e > 0 \quad (27)$$

where

$$\Delta N_{i1} = N_1 - N_i = -\Delta N_{1i} \quad (28)$$

Thus in this case,

$$M_0 = \frac{2V_{\Delta N1i}^T P(I-H)e}{V_{\Delta N1i}^T PV_{\Delta N1i}} > 1 \quad (29)$$

and,

$$M_1 = \frac{2V_{\Delta N1i}^T PV_1}{V_{\Delta N1i}^T PV_{\Delta N1i}} = \frac{2V_{\Delta N1i}^T P(-V_{\Delta N1i} + V_i)}{V_{\Delta N1i}^T PV_{\Delta N1i}} = -2 + M_0 > -1 \quad (30)$$

Comparing Eqs. (24) and (29), the reason for fixing to wrong ambiguity is clearly illustrated. When the projection of the residual vector of the true error e to the direction of $V_{\Delta N1i}$ is too large which causes $M_0 > 1$, a mis-fixing happens.

Now let us compare Eqs. (24) and (30). M_1 obeys a normal distribution for both cases. In case 1 when $N_0 = N_1$, M_1 ($M_1 = M_0$) obeys a zero mean normal distribution (representing a correction ambiguity vector). In case 2, M_1 obeys a normal distributions with a mean of -2 (representing an incorrect ambiguity vector), as shown in Fig. 2. With given M_1 calculated, a threshold $-1 + k2$ can be set up to decide if M_1 belongs to case 1 or case 2. When

$$M_1 > -1 + k2 \quad (31)$$

we consider M_1 belongs to case 1. Otherwise, we consider M_1 belongs to case 2. Thus M_1 can be considered as an index for ambiguity mis-fixing judgement.

For a given $k2$, the success probability P_s, the mis-fixing probability P_m, and undecided probability P_u can be calculated using Eq. (32), where P_{M1} is the probability distribution function of M_1.

$$\begin{cases} P_s = \int_{-1+k2}^{\infty} P_{M1} dx, & M_1 = M_0 \\ P_m = \int_{-1+k2}^{\infty} P_{M1} dx, & M_1 = -2 + M_0 \\ P_u = 1 - P_s - P_m \end{cases} \quad (32)$$

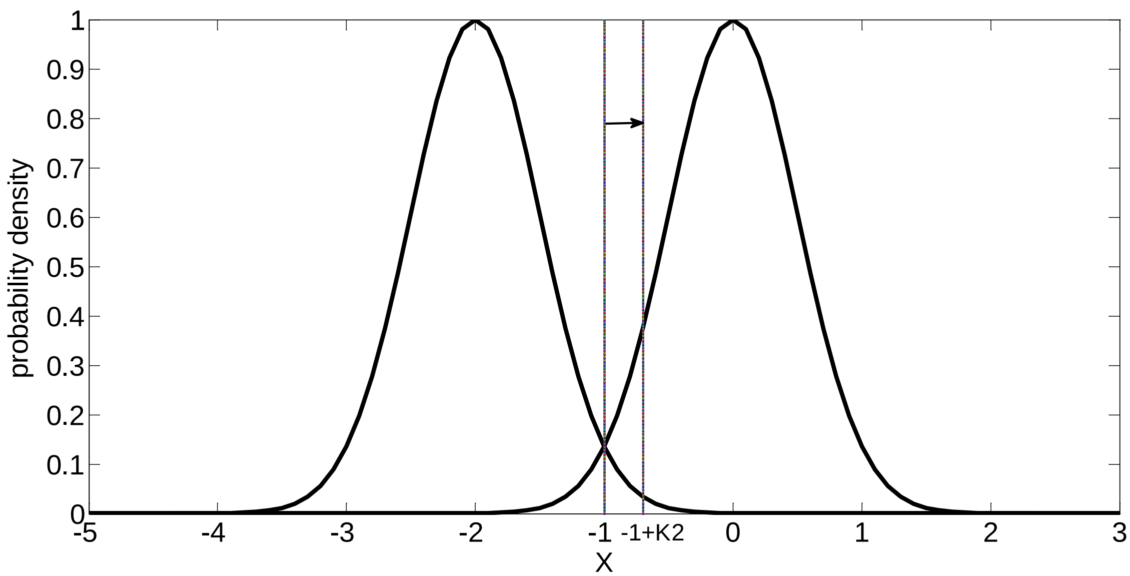

Fig 2 The distribution of M_1 in case 1 and case 2

As shown in Eq. (32), by giving the mis-fixing probability P_m, the threshold $k2$ is uniquely determined with the given variance of M_0. Assuming the true error e obeys a normal distribution, M_0 also obeys a normal distribution. The variance of M_0 can be estimated as,

$$\sigma_{M_0}^2 = \left(\frac{2V_{\Delta N1i}^T P(I-H)}{V_{\Delta N1i}^T P V_{\Delta \mathrm{N}1i}}\right)(e \cdot e^T)\left(\frac{2V_{\Delta N1i}^T P(I-H)}{V_{\Delta N1i}^T P V_{\Delta \mathrm{N}1i}}\right)^T \quad (33)$$

Since $e \cdot e^T = \sigma_0^2 P^{-1}$

$$\sigma_{M_0}^2 = \frac{4\sigma_0^2 V_{\Delta N1i}^T P(I-H)P^{-1}(I-H)^T P V_{\Delta \mathrm{N}1i}}{\left(V_{\Delta N1i}^T P V_{\Delta \mathrm{N}1i}\right)^2} = \frac{4\sigma_0^2 V_{\Delta N1i}^T P(I-H) V_{\Delta \mathrm{N}1i}}{\left(V_{\Delta N1i}^T P V_{\Delta \mathrm{N}1i}\right)^2} = \frac{4\sigma_0^2}{V_{\Delta N1i}^T P V_{\Delta \mathrm{N}1i}} \quad (34)$$

Let $\sigma_0^2 \approx \frac{V_1^T P V_1}{d}$, where d is the degree of freedom of Eq. (9). Insert the equation above and Eq. (21) into (34),

$$\sigma_{M_0}^2 \approx \frac{4}{d \bullet S_{1i}} \quad (35)$$

According to Eq. (35), giving a S_{1i}, we can obtain the variance of M_0 ($\sigma_{M_0}^2$). With a given mis-fixing probability P_m and $\sigma_{M_0}^2$, the threshold $k2$ can be uniquely determined.

3. A Geometry Based Ambiguity Validation (GBAV) method

Based on the analysis in section 2, we propose a new ambiguity resolution method using both the geometrical separability condition (Eq. (22)) and the mis-fixing condition (Eq. (31)). Using both conditions, it enables to control the degree of spatial separability of the ambiguity candidates, and to control the probability of mis-fixing rates at the same time.

The ambiguity validation procedure based on the proposed GBAV method can be summarized as:

1) To avoid the big effect on the ambiguity validation of the pseudo-range noise, the GBAV method proposed in this paper is only based on the carrier phase observation. Theoretically, integer hypotheses should be followed from an ILS estimation based on Eq. (5). However, this equation is rank deficient with one epoch observation and thus long times observation will be required to get the float solutions and the ambiguity candidates. As a result, in this study, we calculate the "float" solution for the ambiguity vector with both pseudo-range and carrier phase observations, then determine the ambiguity candidate search space using the LAMBDA method. After the search range of ambiguity is determined, only carrier phase measurements will be used.
2) Check the data quality by examining residual V_1 with various receiver autonomous integrity monitoring (RAIM) fault detection and exclusion (FDE) methods (Feng et al. 2009) and remove measurements if a large error is detected. In this way, some outliers can be detected and removed from observation.

   Repeat 1) and 2) until no more errors can be found.
3) Confirm if the ambiguity vector associates with the smallest sum of residuals is the correct ambiguity, by checking ambiguity vectors with minimum and second minimum sum of residuals satisfying the separability condition (Eq. (22)), mis-fixing condition (Eq. (31)) or not,
4) If 3) are not satisfied, add one more epoch and then repeat 1) and 4).
5) When both separability condition and mis-fixing condition are satisfied, we fix the ambiguity $N_1 = N_0$.

For most conventional ambiguity validation methods (i.e. the ratio test), only one threshold is used. In GBAV algorithm, we applied two thresholds to control spatial separability and mis-fixing probability separately. The crucial issues for GBAV is the selection of the threshold $k1$ and $k2$.

For separability index S_{1i}, if we set the significant level $\alpha = 0.05$, we can estimate the threshold $k1$ with the degree of freedom d (or the number of observations v) using a F-distribution. Fig 3 gives the threshold values of $k1$ with different number of observation from 5 to 31. From Fig 3 we can see the thresholds decrease from 5.05 to 3.79 sharply when the number of observation changes from 5 to 7. When the number of observation is larger than 24, the value of F varied slowly, which is always below 2.0. Thus we simply set a table for $k1$ thresholds with different numbers of observations (Table 1). To balance the reliability and efficiency, the value of $k1$ we selected are all slightly higher than that of the corresponding values from the F distribution.

Table 1 $k1$ thresholds applied in this paper under the significant value of 0.05

v	5	6	7	8~9	10~13	14~23	>24
$k1$	5.5	4.5	4.0	3.5	3.0	2.5	2.0

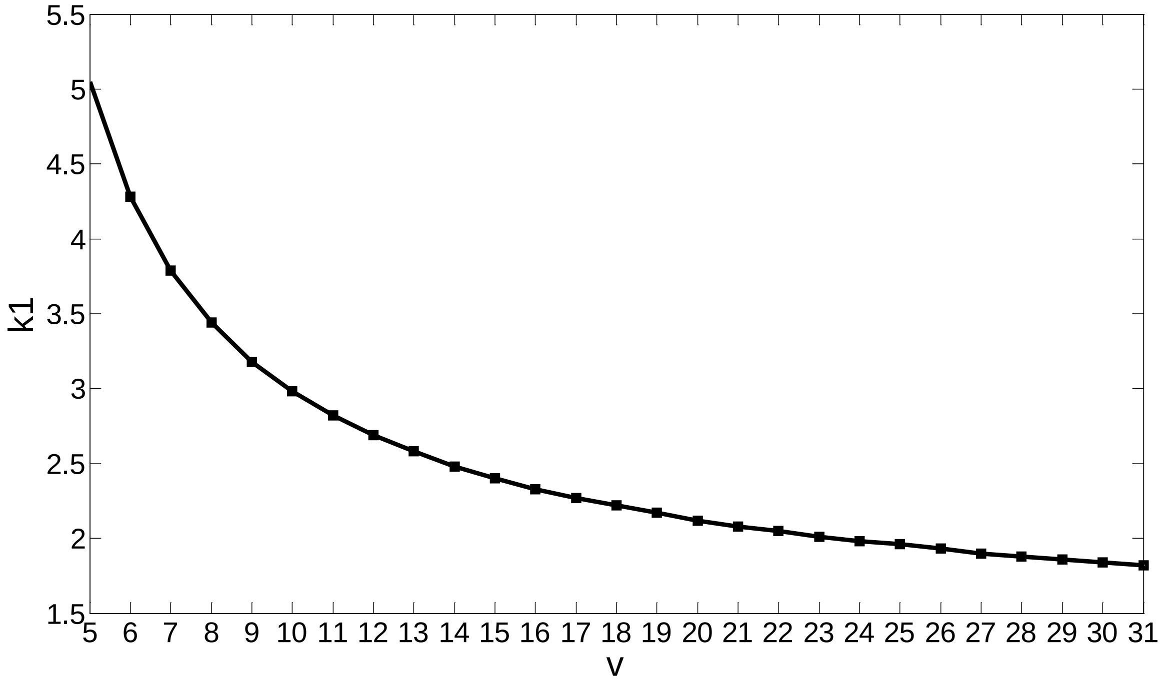

Figure 3 The thresholds of k1 with different number measurements under the significant value of 0.05

To determine the thresholds of $k2$, we need to estimate the variance of M_0 (Eq. (35)) first. We use $k1$ (low bound of S_{1i}) to replace S_{1i} in Eq. (35) and σ_M^2 for different number of observation are given in Table 2. From Table 2, we can find that σ_M^2 decrease steadily from 0.40 to 0.08 when number of observation increase from 5 to 31. Using the largest σ_M^2 which is 0.40 as an example, we can determine the threshold $k2$ with different mis-fixing probability. Table 3 illustrates the thresholds of $k2$, the probabilities of the success and undecided cases when $k2$ is equal to 0 or the mis-fixing probability is set to be 0.1% and 0.01%. As shown in Table 3, the estimation of $k2$ increases considerably from 0.00 to 0.49 when the mis-fixing rate declines. At the same time, the success rate decreases sharply from 99.38% to 90.00%, which means more time will be required to realize the ambiguity resolution when the mis-fixing probability reduces. It should be noted that the values provided here give the upper limits of mis-fixing probability. If the same thresholds are used, with lower value of σ_M^2, the mis-fixing probability will be less than that listed in Table 3.

Since the R-ratio test is very popular and widely used, we compare the GBAV method with it. The R-ratio test is defined as:

$$Ratio = \frac{V_2^T P V_2}{V_1^T P V_1} > k \quad (36)$$

Substituting Eqs. (22) and (24) into (36) yields

$$Ratio = 1 + S_{12} + S_{12} M_1 \quad (37)$$

Table 2 σ_M^2 for different numbers of observation

v	σ_M^2	v	σ_M^2	v	σ_M^2
5	0.40	14	0.15	23	0.10
6	0.31	15	0.14	24	0.10
7	0.26	16	0.13	25	0.09
8	0.23	17	0.13	26	0.09
9	0.21	18	0.12	27	0.09
10	0.19	19	0.12	28	0.09
11	0.18	20	0.11	29	0.08
12	0.17	21	0.11	30	0.08
13	0.16	22	0.10	31	0.08

It can be seen from Eq. (37) that the ratio test is a mixed parameter of spatial separation and mis-fixing index. By giving the thresholds of $k1$ and $k2$, we can obtain ratio test threshold k, which is a function of number of observation and mis-fixing probability. If we select $k1$ in Table 1, and $k2$ =0.0, 0.24 and 0.49 respectively, the thresholds for the R-ratio test varies from 1.00 to 3.20 for the number of observation from 5 to 24 (Table 4).

Table 3 The threshold of $k2$, success and undecided probabilities with $\sigma_M^2 = 0.4$

σ_M	$k2$	-1+$k2$	Success	Undecided	Mis-fixing
0.4	**0.00**	-1.00	99.38%	0.00%	0.62%
0.4	**0.24**	-0.76	97.19%	2.71%	**0.10%**
0.4	**0.49**	-0.51	90.00%	9.99%	**0.01%**

Table 4 The relationship between the thresholds for V-Ratio and GBAV test

$k2$	5	6	7	8~9	10~13	14~23	>24
0.00	1.00	1.00	1.00	1.00	1.00	1.00	1.00
0.24	2.32	2.08	1.96	1.84	1.72	1.60	1.48
0.49	3.20	2.80	2.60	2.40	2.20	2.00	1.80

Even we can use the variable thresholds of the ratio test for ambiguity validation, the GBAV method will be better that the ratio test. For example, in the case when S_{1i} is too small but M_1 is sufficiently large, the result will pass the ratio test. However, in this case, the ambiguity vectors are not spatially separable. Also, when is S_{1i} is very large, but M_1 is too small, the result will also pass the ratio test. But a mis-fixing case would be found with the GBAV method.

4. Numerical Examples

In this section, to evaluate the performance of the GBAV method proposed in this paper, three GNSS data sets with 24-hour observations are used for ambiguity resolutions. According to analyze in Ji and Xu (Ji et al.), we found that a better ambiguity resolution performance will be adopted when the cut off angle of BDS GEOs is set to 20°, and the cut off angle of IGSOs, MEOs is set to 15°. As a consequence, we set the cutoff angle for GEOs to be 20°, and the IGSOs, MEOs, as well as the GPS satellites to be 15°. In addition, the full ambiguity resolution rather than the partial ambiguity resolution is applied. Three ambiguity validation methods are used for ambiguity resolution, namely constant threshold for the ratio test, variable threshold for the ratio test (Eq. (37)), and the GBAV method. The quality of an ambiguity validation method is described by two factors, i.e. time required for ambiguity resolution and ambiguity mix-fixing rate. The first factor indicates the efficiency and the second factor represents the reliability of the validation method.

4.1 Data and Data processing methods

Two short baselines with GPS observation (GODE – GODN, 40 m baseline) and (HARB – HRAO, 1.24 km baseline) from the International GNSS Services (IGS) network, and a middle-range baseline (GS01 – GS02, 30.6 km in Beijing, China) with GPS/BDS observation were used for the evaluation of the GBAV method. For all stations, dual frequency geodetic receivers were installed at the stations. And the observation periods for all baselines are 24 hours. For the two short baselines, the update rate is 30s and for the middle range baseline the update rate is 1s.

To evaluate the performance of the proposed ambiguity validation method, we started from every epoch in the data sets until all ambiguities were fixed to their integers. In data processing, the ambiguity-fix rate (AFR) (Ji et al. 2010) is used to quantify the efficiency performance of ambiguity resolution with the following definition,

$$AFR = \frac{\text{Number of epoch with ambiguity fixed to integer}}{\text{Total number of epochs observed in the data sets}} \quad (38)$$

Also, all mis-fixing cases were recorded and quantified as the percentage of total observed epochs during the 24 hour observation period. In the data processing, we did not estimate σ_M^2 every epoch. Instead, we used the largest value of 0.4 for all processing. To set a baseline for comparison, we used the fixed R-ratio of 1, 1.5, 2.0, 2.5, 3.0, and 3.5. Then for the GBAV method, the thresholds of $k1$, and $k2$, are adopted from Tables 1 and 3. For the variable R-ratio test (Eq. (37)), the thresholds are given in Table 4. It is worth mentioning that, the observation of both GPS and Beidou for all the baselines is double-frequency signals. So the number of the observation in Tables 1 and 4 is generally larger than 8.

4.2 Test results

Baseline 1 (GODE – GODN, 40m)

This is a very short baseline and most of the errors can be effectively cancelled by double differencing. Table 5 gives the ambiguity resolution results with the fixing threshold ratio test. As shown in the table, when the ratio is large than 3.0, there is no mis-fixing case, and the time required for all epochs ambiguity fixed are 5-8 epochs or 3-4 min. More than 97% of epochs the ambiguities can be fixed within one epoch. On the other hand, with the ratio threshold less than 2.5, there are some mis-fixing cases.

The results with variable ratio test and the GBAV method are given in Table 6. When $k_2 = 0.00$, the threshold of R-ratio should be 1.0, and only 1 epoch is needed to fix the ambiguities, which is more efficient than that of the GBAV test. However, the mis-fixing rate (0.14%) is significant higher than that of the GBAV method (0.07%). Since there are 2880 epochs, 4 of them are mis-fixed shown as Table 7. The values of S and M at the first epoch when the Ratio suffer from a mis-fixing are shown in Table 8. It is shown that the values of S in the first, third and last cases are smaller than K1, which means the ambiguity candidates of these cases cannot be spatial separated. When the GBAV test is involved, $k2 = 0.00$, the ambiguities of the last two cases in Table 8 are fixed to the right ones. When $k2$=0.24, the first two cases in Table 8 also achieve the ambiguity resolution correctly, since the M controls the mis-fixing probability. On the other hand, there are 2 epochs (0.07%) of mis-fixing cases using the variable ratio test when $k2$ =0.24 and 0.49 respectively. Take $k2$ =0.49 for instance, the time required for all epoch's ambiguity fixed are 5 to 8 epochs or 2.5 to 4.5 min with the GBAV method. And the variable ratio only need 5 epochs. If we just check one epoch data, the variable ratio method can fix 99% of epochs while the GBAV method can fix around 91% when $k2$ =0.49. Thus, the ratio methods are more efficient than the GBAV method on ambiguity resolution.

Table 5 AFR and Mis-fixing rate of *R*-ratio test with certain values of threshold (GODE – GODN, 40m)

T_f	***Fix R*-ratio AFR (%)**					
	$k = 1$	$k = 1.5$	$k = 2.0$	$k = 2.5$	$k = 3.0$	$k = 3.5$
1	100.00	99.69	99.24	98.72	97.53	96.56
2		100.00	99.90	99.76	99.41	98.89
3			99.93	99.90	99.65	99.31
4			100.00	99.97	99.69	99.44
5				100.00	99.72	99.48
>5 & ≤ 8					100.00	100.00
Mis-fixing rate(%)						
	0.14	0.14	0.07	0.03	0.00	0.00

Note: $\mathbf{T_f}$ stands for Time to fix (epoch)

Table 6 AFR and mis-fixing rate of GBAV and variable *R*-ratio test with varying threshold (GODE – GODN, 40m)

T_f	***Variable R*-ratio AFR (%)**			**GBAV AFR (%)**		
	$k2 = 0.00$	$k2 = 0.24$	$k2 = 0.49$	$k2 = 0.00$	$k2 = 0.24$	$k2 = 0.49$
1	100.00	99.51	99.24	99.48	98.23	91.74
2		99.93	99.86	99.76	99.62	97.67
3		99.97	99.93	100.00	99.72	98.26
4		100.00	99.97		99.93	99.10
5			100.00		100.00	99.38
>5 & ≤ 8						100.00
Mis-fixing rate(%)						
	0.14	0.10	0.07	0.07	0.00	0.00

Table 7 Mis-fixing cases for ratio test (GODE – GODN, 40m)

GPS Time			$k2 = 0.00$ / 1epoch		$k2 = 0.24$		$k2 = 0.49$	
h	m	s	K	ratio	K	ratio	K	ratio
13	25	30	1.00	1.502	1.72	2.382	2.20	3.780
13	29	30	1.00	1.533	1.84	2.163	2.40	5.620
13	55	30	1.00	3.654	1.84	3.654	2.40	3.654
17	25	00	1.00	2.786	1.84	2.786	2.40	2.786

Table 8 Mis-fixing cases for GBAV test (GODE – GODN, 40m)

GPS Time			K1	1 epoch			$k2 = 0.00$		$k2 = 0.24$	
h	m	s		Ratio	S	M	S	M	S	M
13	25	30	3.0	1.502	2.488	-0.798	5.603	-0.863	9.068	-0.119
13	29	30	3.5	1.533	7.966	-0.933	7.966	-0.933	4.484	-0.616
13	55	30	3.5	3.654	2.904	-0.086	9.297	0.086	9.297	0.086
17	25	00	3.5	2.786	2.480	-0.280	7.307	-0.380	7.307	-0.380

Baseline 2 (HARB – HRAO, 1.2 km).

Again, we applied the fix ratio test first and the results are given in Table 9. In this example, for the fix ratio method, when the ratio is larger than 3.5, there are no mis-fixing cases. The time required for all epochs fixed are less than 25 epochs or 12.5 min.

When we use the GBAV method with $k2$=0.49, there are no mis-fixing case and the time required for all epochs fixed are less than 15 epochs or 7.5 min (Table 10). The variable ratio test can fix ambiguity for all epochs during the same period, but there are 3 epochs of mis-fixing (0.10%). On the other hand, for the efficiency of ambiguity fixing, variable ratio test is slightly better.

Baseline 3 (GS01 – GS02, 30.6 km).

As this dataset include both GPS and Chinese BeiDou data, we consider two cases here: GPS only and GPS/BDS data. When we only use GPS data, the results are summarized in Tables 11 and 12. With the fix ratio test, the threshold with no mis-fixing cases is 3.5, and 15 min to resolve ambiguities for all epochs. When $k2$=0.24 and 0.49, the GBAV method can fix ambiguity with no mis-fixing cases. However, the variable ratio test suffers from 7.35% and 1.35% mis-fixing rate when $k2$=0.24 and 0.49. Again, for the efficiency of ambiguity fixing, the variable ratio test is slightly better.

Table 9 AFR and Mis-fixing rate of *R*-ratio test with certain values of threshold (HARB – HRAO, 1.24Km)

T_f	***Fix R*-ratio AFR (%)**					
	$k = 1.0$	$k = 1.5$	$k = 2.0$	$k = 2.5$	$k = 3.0$	$k = 3.5$
≤ 1	100.00	89.97	87.85	81.35	78.09	71.18
≤2		93.47	93.19	88.68	88.44	82.26
≤3		95.03	94.65	91.70	91.39	86.73
≤4		95.66	95.42	93.54	92.78	89.13
≤10		99.41	99.34	98.85	98.68	97.12
≤25		100.00	100.00	100.00	100.00	100.00
Mis-fixing rate(%)						
	8.33	3.47	0.49	0.10	0.03	0.00

Table 10 AFR and mis-fixing rate of GBAV and *R*-ratio test with varying threshold (HARB – HRAO, 1.24Km)

T_f	***Variable R*-ratio AFR (%)**			**GBAV AFR (%)**		
	$k2 = 0.0$	$k2 = 0.2$	$k2 = 0.4$	$k2 = 0.0$	$k2 = 0.2$	$k2 = 0.4$
≤1	100.00	89.03	85.97	90.91	80.10	72.36
≤2		93.51	89.03	99.79	88.23	83.37
≤3		95.03	89.03	100.00	91.84	86.67
≤4		95.63	93.58		92.95	88.72
≤10		99.38	99.06		98.37	95.83
≤15		100.00	100.00		100.00	100.00
Mis-fixing rate(%)						
	8.33	**0.31**	**0.10**	**4.20**	**0.07**	**0.00**

Table 11 AFR and Mis-fixing rate of *R*-ratio test with certain values of threshold (GS01 – GS02, 30.6 km, GPS only)

T_f		***Fix R*-ratio AFR (%)**					
		$k = 1$	$k = 1.5$	$k = 2.0$	$k = 2.5$	$k = 3.0$	$k = 3.5$
0	1	100.00	26.51	7.24	2.28	0.62	0.20
≤1	60		68.32	32.68	11.62	2.72	0.40
≤3	180		81.88	65.72	51.34	33.07	23.96
≤5	300		90.66	77.03	65.65	58.41	45.00
≤10	600		100.00	100.00	99.36	86.16	71.21
≤13	780				100.00	99.32	83.26
≤15	900					100.00	100.00
Mis-fixing rate(%)							
		49.98	22.38	6.16	0.15	0.05	0.00

Table 12 AFR and mis-fixing rate of GBAV and *R*-ratio test with varying threshold (GS01 – GS02, 30.6 km, GPS only)

T_f		***Variable R*-ratio AFR (%)**			**GBAV AFR (%)**		
		$k2 = 0.00$	$k2 = 0.24$	$k2 = 0.49$	$k2 = 0.00$	$k2 = 0.24$	$k2 = 0.49$
0	1	100.00	25.83	5.33	15.70	11.37	0.18
≤1	60		62.76	22.69	72.96	15.43	0.29
≤3	180		72.65	60.56	92.21	47.63	23.02
≤5	300		86.30	70.38	96.16	63.21	42.25
≤10	600		100.00	99.62	100.00	86.33	70.23
≤ 13	780			100.00		100.00	82.06
≤ 15	900						100.00
Mis-fixing rate(%)							
		49.98	7.35	1.56	40.49	0.00	0.00

For the same baseline, the ambiguity resolution performance is much better when using both GPS/BeiDou data (Table 13 and 14). With the fix ratio test (Table 13), when the threshold is larger than 2.5, there are no mis-fixing cases and the time required for 100% ambiguity fixing is only about 30 epochs or 0.5 min. When the variable ratio test and the GBAV method apply (Table 14), there are no mis-fixing cases when $k2$=0.49. The time require for 100% epoch ambiguity fixing is only 15s.

Table 13 AFR and Mis-fixing rate of R-ratio test with certain values of threshold (GS01 – GS02, 30.6 km, GPS+ BDS)

T_f		***Fix R*-ratio AFR (%)**					
		$k = 1$	$k = 1.5$	$k = 2.0$	$k = 2.5$	$k = 3.0$	$k = 3.5$
0	1	100.00	90.42	90.31	86.55	75.12	57.20
≤1/30	2		96.08	96.08	92.65	81.71	63.71
≤1/12	5		99.35	99.35	96.52	87.15	70.99
≤1/6	10		100.00	100.00	98.26	90.20	76.14
≤1/4	15				99.18	92.11	79.20
≤1/2	30				100.00	94.99	84.29
≤4	240					100.00	100.00
Mis-fixing rate(%)							
		8.63	0.12	0.05	0.00	0.00	0.00

Table 14 AFR and mis-fixing rate of GBAV and *R*-ratio test with varying threshold (GS01 – GS02, 30.6 km, GPS+ BDS)

T_f		***Variable R*-ratio AFR (%)**			**GBAV AFR (%)**		
		$k2 = 0.00$	$k2 = 0.24$	$k2 = 0.49$	$k2 = 0.0$	$k2 = 0.24$	$k2 = 0.49$
0	1	100.00	90.53	87.72	72.08	85.38	60.26
≤ 1/30	2		96.08	94.33	90.71	90.46	81.13
≤ 1/12	5		99.35	97.58	100.00	93.88	89.68
≤ 1/6	10		100.00	99.69		100.00	92.57
≤ 1/4	15			100.00			100.00
		8.63	0.05	0.00	4.31	0.00	0.00

From the above examples, we can see that when the threshold is high enough, the fix ratio test can achieve no mis-fixing case for all the test data. However, for different datasets, the thresholds vary from 2.5-3.5. If we use 3.5 for all the cases, it required almost 8 times more observation time for fixing ambiguity for all epochs than that with the threshold of 2.5 in the GPS/BDS case (Table 13). When the GBAV method is used, with $k2$=0.49, there is no mis-fixing case for all the datasets tested. This demonstrates that the GBAV method can effectively control mis-fixing probability. With the variable ratio method, the ambiguity fixing efficiency is generally better that that of the GBAV method, but there are a number of cases of mis-fixing on the three baselines with GPS only observation.

5. Conclusions

In this paper, we introduced two new concepts for ambiguity validation, i.e. spatial separability condition S_{1i} and mis-fixing condition M_1. By using these two concepts, we can understand why ambiguity mis-fixing occurs. If the satellite geometry is not strong enough, there may be a few ambiguity combinations which are not be able to be separated under the existing measurement noise level. Moreover, if the projection of true measurement error residuals to the direction of $V_{\Delta N1i}$ is too large which causes M_0>1, an ambiguity mis-fixing happens. The conventional ambiguity validation methods, such as ratio test and difference test, are the combinations of spatial separability condition S_{1i} and mis-fixing condition M_1. The distributions of S_{1i} and M_1 can be strictly defined which are the functions of the measurement quality, the number of observed satellites, and the satellite geometry. This enables us to set up the thresholds based on user requirements for the quality control the quality of ambiguity resolution.

Based on these concepts, we proposed a new geometry based ambiguity validation (GBAV) method which will ensure different ambiguity combinations to be both geometrically separable and mis-fixing probability controlled. The distributions and threshold computation methods for S_{1i} and M_1 are given in the paper, with given a significant value for S_{1i} and a mis-fixing probability for M_1.

The thresholds for the traditional ratio and difference tests are normally determined empirically as the statistical distributions are difficult to obtain. In this paper, we have shown that the traditional ratio and difference tests are the mixture of spatial separability condition and mis-fixing condition. By applying the same concepts, we can calculate the variable thresholds for the both methods, with given observation number and mis-fixing probability. However, with these single threshold methods, it is possible to have some mis-fixing cases when two ambiguity vectors are not geometrically separable, or M_0 is too small.

To evaluate the performance of the proposed GBAV method, three GNSS datasets with 24-hour observation are processed, using the fix and variable threshold ratio tests as a comparison. It is found that to achieve no mis-fixing for all epochs, the thresholds for different datasets are different. If the thresholds are increased too high, the efficiency of ambiguity resolution can drop significantly. Using the concepts proposed by this paper, when we select the mis-fixing probability less than 0.01% (or $k2$=0.49), there is no mis-fixing case with the GBAV method for all three datasets. However, there are a few cases of mis-fixing for the variable ratio test. On the other hand, the ambiguity fixing efficiency for the variable ratio test is slightly better than that of the GBAV method.

Also, combining GPS/BDS systems, the ambiguity resolution performance can be significantly improved for medium-range baselines. For a 30 km baseline, it requires 15 min for all epoch ambiguity fixed with GPS data only. With GPS/BDS data, the time for all epoch ambiguity fixed can be reduced to 15s.

Acknowledgments

This research was supported by the University Grants Committee of Hong Kong under the scheme of Competitive Earmarked Research Grant (Project No: 152223/18E) and the research fund from the Smart Cities Research Institute, Hong Kong Polytechnic University.

References

Euler HJ, Landau H (1992) Fast GPS ambiguity resolution on-the-fly for real-time applications. In: Proceedings of 6th Int. Geod. Symp. on satellite Positioning, Columbus, Ohio. pp 650–659

Euler H-J, Schaffrin B (1991) On a measure for the discernibility between different ambiguity solutions in the static-kinematic GPS-mode. In: Kinematic Systems in Geodesy, Surveying, and Remote Sensing. Springer, pp 285–295

Feng S, Ochieng W, Moore T, et al (2009) Carrier phase-based integrity monitoring for high-accuracy positioning. GPS Solut 13:13–22.

Frei E, Beutler G (1990) Rapid static positioning based on the fast ambiguity resolution approach FARA: theory and first results. Manuscripta Geod 15:325–356.

Han S (1997) Quality-control issues relating to instantaneous ambiguity resolution for real-time GPS kinematic positioning. J Geod 71:351–361.

Han S, Rizos C (1999) The impact of two additional civilian GPS frequencies on ambiguity resolution strategies. In: 55th National Meeting US Institute of Navigation, “Navigational Technology for the 21st Century”, Cambridge, Massachusetts. pp 28–30

Hofmann-Wellenhof B, Lichtenegger H, Collins J (1993) Global Positioning System. Theory and Practice. Springer-verlag

Ji S, Chen W, Ding X, et al (2010) Ambiguity validation with combined ratio test and ellipsoidal integer aperture estimator. J Geod 84(10):597–604.

Ji S, Wang X, Xu Y, et al (2014) First Preliminary Fast Static Ambiguity Resolution Results of Medium-Baseline with Triple-Frequency Beidou Wavebands. J Navig 67(6): 1109-1119

Leick A (2004) GPS satellite surveying. John Wiley & Sons

Li T, Wang J (2012) Some remarks on GNSS integer ambiguity validation methods. Surv Rev 44:230–238.

Parkinson B, Spilker JJ, Axelrad P, Enge P (1996) GPS: theory and applications, vols 1 and 2. American Institute of Aeronautics and Astronautics

Teunissen PJG (1995) The least-squares ambiguity decorrelation adjustment: a method for fast GPS integer ambiguity estimation. J Geod 70(1-2):65–82.

Teunissen PJG (1999) An optimality property of the integer least-squares estimator. J Geod 73(11):587–593.

Teunissen PJG (2013) GNSS integer ambiguity validation: overview of theory and methods. Proc Inst Navig Pac PNT 673–684.

Teunissen PJG (2003) A carrier phase ambiguity estimator with easy-to-evaluate fail-rate. Artif Satell 38:89–96.

Teunissen PJG (2004) Penalized GNSS ambiguity resolution. J. Geod., 78(4-5):235–244.

Teunissen PJG (1998) On the integer normal distribution of the GPS ambiguities. Artif Satell 33:49–64.

Teunissen PJG (2000) ADOP based upperbounds for the bootstrapped and the least-squares ambiguity success rates. Artif Satell 35:171–179.

Teunissen PJG (2005) Penalized GNSS ambiguity resolution with optimally controlled failure-rate. Artif Satell 40:219–227.

Teunissen PJG, Verhagen S (2009) The GNSS ambiguity ratio-test revisited: a better way of using it. Surv Rev 41(312):138–151.

Teunissen PJG, Verhagen S (2004) On the foundation of the popular ratio test for GNSS ambiguity resolution. In: Proc. ION GNSS. pp 2529–2540

Tiberius C, De Jonge PJ (1995) Fast positioning using the LAMBDA method. Proc. DSNS 95, Norway, Paper No. 30

Verhagen S (2004) Integer ambiguity validation: An open problem? GPS Solut 8:36–43.

Verhagen S (2005) On the reliability of integer ambiguity resolution. Navigation 52:99–110.

Verhagen S, Teunissen PJ (2013) The ratio test for future GNSS ambiguity resolution. GPS Solut 17:535–548.

Verhagen S, Teunissen PJ (2006) New global navigation satellite system ambiguity resolution method compared to existing approaches. J Guid Control Dyn 29:981–991.

Wang J, Stewart MP, Tsakiri M (1998) Stochastic modeling for static GPS baseline data processing. J Surv Eng 124:171–181.

Xu PL, Cannon E, Lachapelle G (1995) Mixed integer programming for the resolution of GPS carrier phase ambiguities, presented at IUGG95 Assembly, Boulder, July 2–14.

Authors

Wu Chen is a Professor at the Department of Land Surveying and Geo-Informatics in the Hong Kong Polytechnic University. His interests include GNSS Applications on Transportation, Kinematic GPS, System Integration, GNSS Performance Evaluation, GPS Software Receiver, Regional GPS Network, Vehicle and Personal Navigation Systems, and Wireless Sensor Network.

Ying Xu is an Associate Professor Shandong University of Science and Technology. She received a PhD degree from the Hong Kong Polytechnic University in 2016. Her research focuses on the algorithm development for high precision GNSS.

Duojie Weng is a Research Assistant Professor with the Hong Kong Polytechnic University. His interests included GNSS, indoor positioning and precise positioning. He received the PhD from the Hong Kong Polytechnic University in 2016, and MSc and BSc degrees in Electrical Engineering from Hohai University in China.

Shengyue Ji is an Associate Professor in China University of Petroleum (East China). His research interests include precise GNSS positioning and the inonosphere in low latitude areas etc. He has published more than 30 papers in international famous journals as the first or corresponding author, such as Journal of Geophysical Research, Journal of Geodesy, GPS Solutions, etc. And he has made scientific contributions many GNSS aspects, such as precise Ocean navigation and positioning, ambiguity resolution and validation, cycle slip detection and repairing, precise point positioning, data quality control etc.